Soft Matter

Accepted Manuscript

This article can be cited before page numbers have been issued, to do this please use: Y. Min and P. K. Purohit, *Soft Matter*, 2018, DOI: 10.1039/C8SM00852C.

ROYAL SOCIETY OF CHEMISTRY

rsc.li/soft-matter-journal

View Article Online
DOI: 10.1039/C8SM00852C

Journal Name

ARTICLE TYPE

Cite this: DOI: 10.1039/xxxxxxxxxx

Discontinuous growth of DNA plectonemes due to atomic scale friction†

Yifei Min,[a] Prashant K. Purohit,[b‡]

Received Date
Accepted Date

DOI: 10.1039/xxxxxxxxxx

www.rsc.org/journalname

We develop a model to explain discontinuities in the increase of the length of a DNA plectoneme when the DNA filament is continuously twisted under tension. We account for DNA elasticity, electrostatic interactions and entropic effects due to thermal fluctuation. We postulate that a corrugated energy landscape that contains energy barriers is the cause of jumps in the length of the plectoneme as the number of turns is increased. Thus, our model is similar to the Prandtl-Tomlinson model of atomic scale friction. The existence of a corrugated energy landscape can be justified due to the close proximity of the neighboring pieces of DNA in a plectoneme. We assume the corrugated energy landscape to be sinusoidal since the plectoneme has a periodic helical structure and rotation of the bead is a form of periodic motion. We perform calculations with different tensile forces and ionic concentrations, and show that rotation-extension curves manifest stair-step shapes under relatively high ionic concentrations and high forces. We show that the jump in the plectonemic growth is caused by the flattening of the energy barrier in the corrugated landscape.

1 Introduction

Twisted DNA and formation of structures like DNA supercoils, which are also known as plectonemes, has been studied both theoretically using elastic rod models[1–7], and experimentally through single molecule experiments[8–12] by many authors. In the experiments, a DNA molecule has one end fixed, while the other end is given a tensile force and is twisted by a certain number of turns. When the number of turns (or linking number) has reached some critical value, the filament jumps from a straight regime into a plectonemic regime. This critical value of linking number has been found to depend on several parameters like temperature, tension, ionic concentration of the solution, etc. Parameters characterizing the plectoneme, such as, the torsional stress, helical radius, slope of rotation-extension curve, and critical number of turns can be measured in the experiments. In theoretical studies, the DNA molecule is modeled as an elastic-isotropic rod. By considering the elasticity of the DNA filament together with the electrostatic and entropic interactions, some models give good quantitative agreement with the experimental data and are able to completely reproduce the rotation-extension curve. Similar agreement between theory and experiment has also been obtained using various molecular simulation methods[10,11].

From previous experiments it is known that after a plectoneme is formed, the rotation-extension curve behaves like a decreasing function in which the extension decreases nearly linearly with rotation of the bead. However, a recent experiment[13] has found that under certain conditions, the rotation-extension curve exhibits a stair-step shape. This means that the end-to-end distance is not necessarily a smooth function of the number of applied turns. Instead, the change in end-to-end distance proceeds in discrete events. Furthermore, within each 'stair' the curve is nearly horizontal, which indicates that the end-to-end distance corresponding to that stair remains unchanged despite the slight increase in the number of turns. If the DNA filament is twisted more, there is a sudden jump in the end-to-end distance, which then starts another stair. Such phenomena are mostly observed in experiments with high tensile forces ($\approx$ 3.5pN) and high ionic concentrations (1M). To the best of our knowledge, this is not predicted by any of the existing models. Some existing models[6,14,15] accurately predict the discontinuities in extension and torque at the plectoneme transition as well as the average slope of the rotation-extension curve, but they say nothing about the periodicity of the torque and the stair-step rotation-extension curve. Here, we propose a new model that takes into consideration the microscopic friction between neighboring pieces of DNA in a plectoneme to explain this stair-step pattern in the rotation-extension curves. A model with some similar features has been suggested

[a] Graduate Group in Applied Mathematics and Computational Science, University of Pennsylvania, Philadelphia, PA 19104, USA. E-mail: minyifei@sas.upenn.edu
[b] Department of Mechanical Engineering and Applied Mechanics, University of Pennsylvania, Philadelphia, PA 19104, USA. Tel.:+215 898 3870; Fax: +215 573 6334. E-mail: purohit@seas.upenn.edu
‡ Graduate Group in Applied Mathematics and Computational Science, University of Pennsylvania, Philadelphia, PA 19104, USA.

View Article Online
DOI: 10.1039/C8SM00852C

by Dittmore and Neuman[13].

Our new model is based on the work in[6] which models DNA as an isotropic rod and accounts for elasticity, electrostatic interaction and entropy due to thermal fluctuation. By adding friction to this model, we can predict the jump behavior in plectonemic growth as a consequence of frictional energy barriers like in the Prandtl-Tomlinson model (or P-T model) of atomic scale friction[16]. Our approach to this problem is different from some earlier works which consider friction in DNA. For example, Poirier *et al.*[17,18] model rate-dependent internal and external dissipation in chromosomes, but friction in their models is due to fluid drag. Ghosal[19,20] considers friction experienced by DNA in a viral capsid, but his model considers a Coulomb-type law of static friction in which the frictional force is proportional to the normal force on the DNA. To our knowledge, this is the first time friction in a DNA plectoneme has been modeled using corrugated energy landscapes that form the basis of the Prandtl-Tomlinson model of atomic scale friction[16].

Our model predicts a non-constant periodically varying torque in the plectonemic regime when applied turns increase. It is known that there are discontinuities in the extension and torque during the transition from the straight to the plectonemic regime, but after this jump occurs previous models predict that the torque in the plectoneme remains constant no matter how many extra turns are added to the DNA. However, recent experiments[13] have found that in the case where the rotation-extension curve has a stair-step shape, the corresponding rotation-torque curve has a periodic behavior which we call a 'stick-slip' pattern. One period in the rotation-torque curve corresponds to a stair in the rotation-extension curve. Within one period, the corresponding torque keeps increasing as more turns are added until a certain critical torque is reached. Upon reaching the critical torque, a sudden jump happens, the torque drops to a lower level, and another 'stair' starts. It is worth mentioning that this critical torque is different from the critical torque at which supercoiling (or plectoneme formation) begins. The former is smaller than the latter. Our newly proposed model explains the mechanism of these phenomena and theoretically predicts the periodicity of the rotation-torque curve and the value of the second critical torque.

2 General theory

The DNA filament is modeled as an inextensible isotropic Kirchhoff rod of length $2L$. The centerline of the rod is defined to be a space curve $\mathbf{r}(s)$ with $-L \le s \le L$where s is the arc length along the centerline. The centerline $\mathbf{r}(s)$ is associated with a right-handed orthonormal basis $\mathbf{d}_i(s)$, $i = 1,2,3$. $\mathbf{d}_3(s) = \mathbf{r}'(s)$ is defined to be the unit tangent vector of the centerline. We define three scalar valued functions $\kappa_i(s)$, $i = 1,2,3$ where κ_1 and κ_2 measure the physical bending such that the curvature is given by $\kappa = \kappa_1^2 + \kappa_2^2$, and κ_3 measures the physical twist. We use the constitutive relation of linear elasticity so that the torque is given by $\mathbf{M} = K_b\kappa_1\mathbf{d}_1 + K_b\kappa_2\mathbf{d}_2 + K_t\kappa_3\mathbf{d}_3$, where K_b is the bending modulus and K_t is the twisting modulus.

We partition the DNA rod into three regions: the tails, the plectoneme, and the loop. The contour length of the two tails is denoted by $L_t = 2l_t$, the contour length in the loop is denoted by L_o,

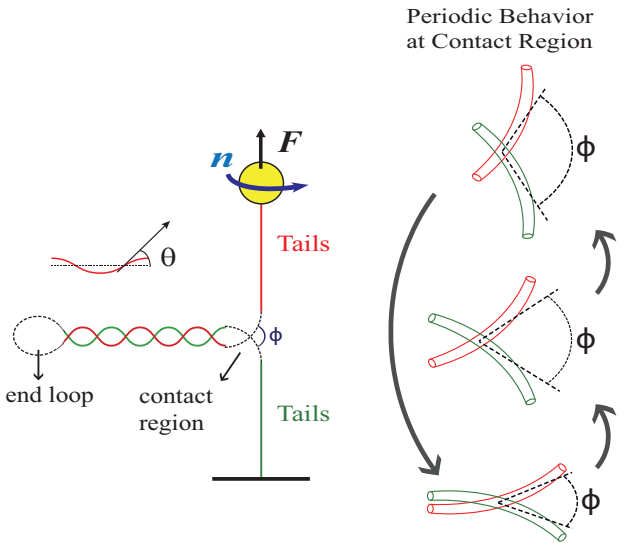

Fig. 1 Sketch representing experiments in which a DNA filament is fixed at one end while the other is subjected to a pulling force F and applied turns n. The tangent angle Φ between two strands in the contact regrion changes periodically as the plectoneme length L_p increases. Thus, the interactions between the two strands in the contact region must also vary periodically as a function of L_p. This may be the origin of a periodic energy landscape that is key to the Prandtl-Tomlinson type model[16] used here to model the discontinuous growth of a DNA plectoneme.

and the contour length of the two helices is denoted by $L_p = 2l_p$. By summing the length of all regions we get $2L = L_t + L_p + L_o$. The helical angle and radius of the plectoneme is denoted by θ and r respectively, and they are assumed not to vary with arc-length s for simplicity. M_3 is defined as the twisting moment when the plectoneme is formed. By conservation of torque about the centerline of an isotropic Kirchoff filament, M_3 is constant along the rod[21].

2.1 Model without friction

We first briefly introduce the model of Argudo and Purohit[6] in which friction is not taken into consideration. For details we refer the reader to section 2 of[6].

The configuration of the rod is fully specified by the centerline through parameters r, θ and M_3. These parameters are computed as functions of the loading (tensile force, F, and number of applied turns, n) by solving an optimization problem of minimizing the free energy of the entire length of DNA.

Let Lk_t, Lk_p, and Lk_o denote the excess link in the tail, in the plectoneme and in the loop, respectively. Let n denote the number of turns imposed on the end of the DNA. Then we have the following constraint on the minimization problem:

$$n = Lk_t + Lk_p + Lk_o. \tag{1}$$

Lk_t consists of the twist together with a writhe due to thermal fluctuation[22]:

$$Lk_t = \frac{M_3 L t}{2\pi}\left(\frac{1}{K_t} + \frac{1}{4K_b K}\right) + O(K^{-3}), \tag{2}$$

View Article Online
DOI: 10.1039/C8SM00852C

where

$$K = \frac{\sqrt{K_b F - M_3^2/4}}{k_B T}. \tag{3}$$

T is the absolute temperature and k_B is the Boltzmann constant. Lk_p is given by[15]

$$Lk_p = \left(\frac{M_3}{2\pi K_t} - \chi\frac{\sin 2\theta}{4\pi r}\right)L_p, \tag{4}$$

where χ stands for the handedness of the helix. Here $\chi = 1$ for a right-handed helix. The link in the end loop of the rod Lk_o is approximated by

$$Lk_o = \frac{M_3 L_o}{2\pi K_t} + Wr_o. \tag{5}$$

We take $Wr_o = 1$ in our computation for simplicity. We express the total free energy in the system as

$$V = V_{tails} + V_{plec} + V_{loop}. \tag{6}$$

The free energy in the tails is given by

$$V_{tails} = \frac{M_3^2}{2K_t}L_t + \frac{M_3^2}{4K_b K}L_t + GL_t - FL_t, \tag{7}$$

Here G is a correction due to thermal effects[22] and is given by

$$G = \frac{(k_B T)^2}{K_b}K\left(1 - \frac{1}{4K} - \frac{1}{64K^2}\right) + O(K^{-3}), \tag{8}$$

where K is the same as in Eq.(3). For the energy in the end loop, we only consider the elastic energy from twisting and bending[23]:

$$V_{loop} = \left(\frac{M_3^2}{2K_t} + F\right)L_o, \tag{9}$$

with $L_o = 4\sqrt{K_b/F}$. The free energy of the plectoneme is divided into two parts:

$$V_{plec} = V_{elas}^{plec} + V_{int}^{plec}. \tag{10}$$

The elastic energy is given by

$$V_{elas}^{plec} = \frac{M_3^2}{2K_t}L_p + \frac{K_b}{2}\frac{\sin^4\theta}{r^2}L_p\ . \tag{11}$$

We write the energy due to internal interaction as $V_{int}^{plec} = U \cdot L_p$. Here $U = U_{conf} + U_{el}$ consists of configurational entropy and electrostatic interactions. The configurational entropy is given by[24–26]:

$$U_{conf}(d_r, \theta) = \frac{k_B T}{A^{1/3}}\left(\frac{c_p}{(p\pi)^{2/3}} + \frac{c_r}{d_r^{2/3}}\right), \tag{12}$$

where $A = K_b/(k_B T)$ is the persistence length of the DNA, $2\pi p$ is the helical pitch with $p = r\cot\theta$, and d_r represents the small undulations of the helix in the radial direction due to thermal effects. The terms c_r and c_p are taken to be $c_r = c_p = 2^{-8/3}$ [26]. For the electrostatic energy we adopt the expression given by Ubbink and Odijk[24] based on the analysis in the supplementary material of[6]:

$$U_{el} = \frac{1}{2}k_B T \nu^2 l_B g(\theta)\sqrt{\frac{\lambda_D \pi}{r}}e^{2\frac{d_r^2}{\lambda_D^2} - \frac{2r}{\lambda_D}}, \tag{13}$$

$$g(\theta) = 1 + 0.83\tan^2(\theta) + 0.86\tan^4(\theta). \tag{14}$$

Here the Debye length λ_D (nm) is given by $\lambda_D = 0.305[nm]/\sqrt{c_o[M]}$, where $c_o[M]$ is the ionic concentration[27]. l_B is the Bjerrum length, which is approximately 0.7 nm in water at $T = 300$ K[27]. ν is the effective linear charge depending on the ionic concentration[10,14] for which we use the value obtained from linear regression $\nu^{fit} = 2.46 + 2.38 \times 10^{-2} c_o$.

2.2 Energy minimization without friction

In the absence of friction, once the DNA filament has transformed from the straight regime into the plectonemic regime, the torque M_3 remains constant. In the presence of friction, we will see that from both the experimental data and theoretical prediction, M_3 will manifest periodic behavior – in each period, it first increases from a fixed critical value to another large critical value, at which a jump happens and it falls back to the first critical value. In each period when M_3 increases, the plectoneme does not grow, i.e., the end-to-end distance remains nearly unchanged.

In the model without friction, to solve for parameters (eg. M_3, r,θ, $\cdots$), we set the following partial derivatives to zero[6,14,15,24,28]:

$$\left\{\frac{\partial V}{\partial M_3}, \frac{\partial V}{\partial r}, \frac{\partial V}{\partial \theta}, \frac{\partial V}{\partial L_p}, \frac{\partial V}{\partial d_r}\right\} = 0. \tag{15}$$

In this framework, the length of the plectoneme L_p and the total link n satisfy a linear relation by Eqs. (1), (2), (4), (5):

$$n = \frac{M_3}{2\pi K_t}L + \frac{M_3}{8\pi K_b K}(L - L_o) + Wr_o + \left(-\chi\frac{\sin 2\theta}{4\pi r} - \frac{M_3}{8\pi K_b K}\right)L_p, \tag{16}$$

with all the parameters except L_p fixed for given tensile force F and ionic concentration c_o. It follows that the end-to-end distance $\triangle z$ is given by[29]:

$$\triangle z = \rho(L - L_o - L_p), \tag{17}$$

where

$$\rho = 1 - \frac{1}{2}\frac{1}{\sqrt{\frac{K_b F}{k_B{}^2 T^2} - \frac{M_3^2}{4k_B^2 T^2} - \frac{1}{32}}} + \frac{K_b k_B T}{L\left(K_b F - \frac{M_3^2}{4}\right)}. \tag{18}$$

We see that ρ is independent of n. Since L is constant and L_o is approximately constant, $\triangle z$ is a nearly linear function of n.

This model performs well under scenarios with moderate force and ionic concentration, when no self-contact between strands is assumed to happen. It predicts that the helical radius r decreases as tensile force and ionic concentration increase. In Fig. 2 we give the theoretical plot of radius as a function of tensile force F at three different values of ionic concentration. The value of radius gradually comes very close to 1 nm as F increases. This indicates that when the tensile force and ionic concentration are

View Article Online
DOI: 10.1039/C8SM00852C

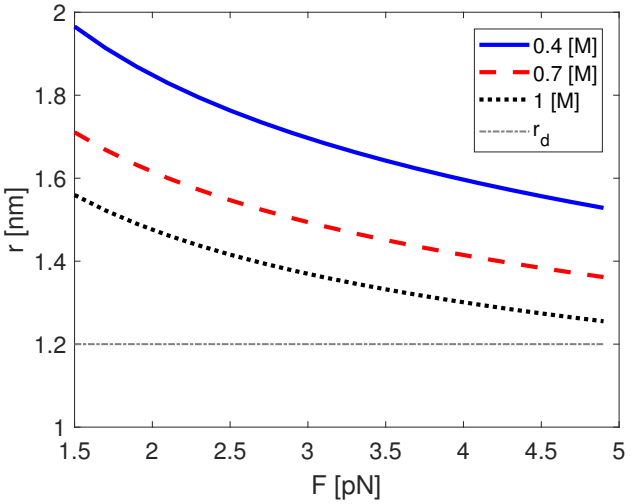

Fig. 2 Theoretical predictions for superhelical radius r for three different ionic concentrations according to the model in [6]. The radius of DNA r_d is marked by the constant gray dash-dot line in the figure. All three curves tend to the gray line as tension F increases, indicating that the distance between strands tends to zero which may lead to friction. In reality, the radius r_d is between 1 and 1.2 nm [30].

sufficiently high, the radius will be small enough to allow physical contact between the two strands of the plectoneme. Indeed, the radius is less than 1.3 nm when tension is 3.5 pN and ionic concentration is 1M (in the experiment by Dittmore and Neuman [13]). The distance of the surface of the two strands is given by $2(r-r_d)$, where r_d is the radius of the isotropic rod in our simplified model for the DNA filament. It is well-known that the value of r_d is between 1 and 1.2 nm [30]. So, a value as small as $r = 1.3$ nm suggests that nearby pieces of DNA in the plectoneme and the contact region (see figure 1) are so close that friction cannot be neglected. In fact, the possibility of slithering motion between neighboring pieces of DNA in a plectoneme being hindered by a rugged energy landscape was recognized by Loenhout *et al.* [31]. In what follows we consider frictional interactions for rotational motion of the DNA at the contact region connecting the plectoneme to the tails.

2.3 Model with friction

The reason why we propose a model with friction is as follows. The experiments of Dittmore and Neuman [13] reveal that within each period of plectonemic growth, the end-to-end distance does not change, and the torque grows until some critical value is reached. This picture is very similar to atomic 'stick-slip' in the P-T model. In the classical 1-dimensional P-T model, a point mass is pulled along a periodic substrate. The substrate is modeled by a periodic, or corrugated, potential energy field [32,33]. The position of the point mass in response to pulling is determined by a minimization of energy. The mass stays in one well and the force increases until a critical value is reached which causes the mass to surmount an energy barrier and jump into the next well. This results in a periodically varying lateral force in the system [16] which is the mechanism behind stick-slip in the P-T model.

The cause of the discontinuities in the P-T model is the corrugated substrate potential energy field [16]. The discontinuous and periodic growth of a DNA plectoneme suggests the existence of a similar potential energy landscape as in the P-T model. This peridoic interaction energy has wells and energy barriers. In response to loads the DNA adopts a configuration in which the energy is at a local minimum. When there is no energy barrier the configuration can change continuously, which means that the plectoneme grows smoothly to maintain a minimum energy state. However, when the barrier is high (several times larger than k_BT), the filament cannot move freely from one local minimum to the next. Although the neighboring local minimum has a smaller total free energy, the system gets stuck in the current local minimum because of the barrier in between. This is the same as the reason for the stick part of the stick-slip motion in the classical P-T model. As for the slip part, it comes from the elimination of the barrier as a consequence of increasing applied turns. It can be shown that during the stick phase, increasing applied turns gradually flattens the energy barrier. When its value comes close to k_BT, the slip is induced due to thermal fluctuation since the barrier is low enough to be surpassed. The length of the plectoneme jumps to the next local minimum, and a new period is started and the whole process described above is repeated.

Unlike the case of the 1-dimensional P-T model, the origin of the periodic energy field in our case is not fully clear, but we offer a possible explanation for how it could arise. We conjecture that frictional interactions hinder the sliding and rotation between two neighboring pieces of DNA in the contact region which connects the tail and the plectoneme (see figure 1). Contact points in DNA supercoiling have been theoretically analyzed by Stump *et al.* [34,35] whose computation shows that there could be sliding of the two strands against each other during the process of plectonemic growth. The angle Φ in this contact region (see figure 1) varies periodically as the length of the plectoneme L_p (or the number of applied turns n) increases. Therefore, the interactions between the two rotating pieces of DNA in this region must also be periodic functions of L_p (or n). A major contribution to this interaction energy must be the electrostatic interaction of the neighboring pieces of DNA at the 'contact point'. This energy depends on both the distance z between the two strands (here the distance is defined to be the shortest distance between two points chosen from two strands) and the angle between them, which is Φ in Fig. 1. If the distance z remains fixed, then the periodic change of Φ implies a periodic change of the electrostatic energy between the two strands. We call the amplitude of this periodic interaction energy U_0. Later we will show that U_0 depends both on the tension F and the ionic concentration c_0.

The idea that a periodic energy landscape is the cause behind the stair-step rotation-extension curves has been suggested also by Dittmore and Neuman [13]. We agree with Dittmore and Neuman that the energy barrier arises because of interactions at the point where the plectoneme joins the tails. In [13] these interactions have to do with symmetries that repeat as the plectoneme is extended by the wavelength λ of a solenoid (or helical) solution of the elastic rod equations given by Thompson and Champneys [36]. Hence, Dittmore and Neuman [13] give the period of this enegry landscape as the solenoid wavelength λ and estimate that its am-

View Article Online
DOI: 10.1039/C8SM00852C

plitude depends on the plectoneme radius r and applied tension F. Since the plectoneme radius depends both on F and the ion concentration c_0, the energy barrier suggested by Dittmore and Neuman[13] shares many qualitative features with our assumptions about U_0 above.

To mathematicize the above description of discontinuous plectoneme growth, let L_p^{crit} denote the critical length of the plectoneme, i.e., the length of the plectoneme at the first transition of the DNA from a straight state into a plectoneme. We define the excess length of the plectoneme $\triangle L_p = L_p - L_p^{crit}$ so that in the plectonemic regime $\triangle L_p \geq 0$. Similarly, let n_{crit} denote the critical link at which the plectonemic transition takes place. Define the excess link $\triangle n = n - n_{crit}$. We will represent the total free energy as a function of $\triangle L_p$ and $\triangle n$. Note that when $\triangle L_p = 0$ and $\triangle n = 0$, we have $n = n_{crit}$ and $L_p = L_p^{crit}$. The system is in the state right after the transition. This means when $\triangle n = 0$, $\triangle L_p = 0$ is a local minimum of the free energy of the system. In the model without friction, there is no background periodic energy field. When more turns are added, i.e., $\triangle n$ increases, $\triangle L_p$ increases simultaneously in order to stay in a local minimum.

By assuming the corrugated energy field to be a sinusoidal function of $\triangle L_p$, we can write the total energy stored in the system as

$$V_{tot}(\triangle Lp, \triangle n) = -U_0 \cos\frac{2\pi\triangle L_p}{a} + V_f(\triangle L_p, \triangle n), \tag{19}$$

where a is a periodicity and $\triangle n$ is the extra turns added. The two components of the free energy in the right hand side of eqn. (19) are plotted separately in Fig. 3a. The quantitative analysis on a is carried out in section 2.4, where we will see that it is related to the amplitude U_0 and the slope of the rotation-extension curve. V_f is the total elastic plus internal energy of the filament given by Eq. (6), which is a function of $\triangle L_p$ and $\triangle n$ since we assume that all the other parameters (θ, r, d_r) are already known by solving the minimization problem. V_f will be described in more detail later. The shape of V_{tot} depends on how many more turns are added (see Fig. 3b). From Fig. 3b, we can see that when $\triangle n = 0$, i.e., a period is just about to start, the first local minimum is located at $\triangle L_p = 0$, which is simply a result from the previous model[6]. The beginning corresponds to the lowest curve in Fig 3b. The extra length of plectoneme is fixed at a minimum of V_{tot}, which is given by the solution of $\partial V_{tot}/\partial\triangle L_p = 0$. We see that there is an energy barrier between the first and the second local minimum. This barrier is several times k_BT, so it prevents movement between minima. As $\triangle n$ increases, the twist results in a growing torque, and the curve of V_{tot} moves upwards as a whole, while the barrier from the first minimum to the second becomes smaller, and is finally flattened (highest curve in Fig. 3b). At non-zero temperature the dynamics of the filament should be taken into consideration. When the barrier from left to right is comparable to k_BT, the filament becomes unstable and it initiates a jump to the next stable length of plectoneme. So far a full period of stick-slip motion is finished, and a new period is about to start.

In order for the stick-slip motion to happen, there are several important conditions that need to be satisfied. First, the corrugated energy landscape, which is the first term on right hand size of Eq. 19, comes from the periodic interaction between the two strands of the plectoneme, which can only happen when they are close to each other. That is why the phenomenon of stick-slip motion of plectonemic growth is only observed under large force and high ionic concentration. Second, the geometry of the function $V_f(\triangle L_p, \triangle n)$ in Eq. 19 determines whether a flattening of the energy landscape is possible. In the classical P-T model, the second term is a quadratic function of the position variable ($\triangle L_p$ in our case), which is convex decreasing around the first local minimum for $\triangle n > 0$[37]. Also, the absolute value of the partial derivative with respect to the position variable should increase as $\triangle n$ increases. This implies that the elastic plus internal energy V_f in Eq. 19 should possess similar properties, i.e., it has to be a convex and decreasing function of $\triangle L_p$, and $|\partial V_f/\partial\triangle L_p|$ increases as excess link $\triangle n$ increases.

In our model, V_f is the total free energy from the model in[6]. So it adopts the same expression as Eq.(6) with some terms modified:

$$V_f(\triangle L_p, \triangle n) = V_{elas}^{plec*} + V_{int}^{plec*} + V_{tails}^{*} + V_{loop}^{*}, \tag{20}$$

where

$$V_{elas}^{plec*} = \left(\frac{M_3^{*2}}{2K_t} + \frac{K_b \sin^4\theta}{2r^2}\right) L_p, \tag{21}$$

$$V_{int}^{plec*} = U * L_p, \tag{22}$$

$$V_{tails}^{*} = \left(\frac{M_3^{*2}}{2K_t} + \frac{M_3^{*2}}{4K_bK^*} + G^* - F\right) L_t, \tag{23}$$

$$V_{loop}^{*} = \left(\frac{M_3^{*2}}{2K_t} + F\right) L_o, \tag{24}$$

where $L_p = L_p^{crit} + \triangle L_p$ and $L_t = L - L_p - L_o$. The length of end loop $L_o = 4\sqrt{K_b/F}$ is fixed since F remains unchanged during the process. Here, θ, r, L_p^{crit} are obtained by solving the energy minimization problem with constraint from the model without friction, i.e., minimizing the energy in Eq. (6) under constraint Eq. (1). $M_3^* = M_3^*(\triangle L_p, \triangle n)$ depends on $\triangle L_p$ and $\triangle n$. To calculate M_3^*, we replace n in Eqn.(1) with $n + \triangle n$, and use the calculated values for θ and r, together with Eqs.(2),(3),(4) and (5). These altogether give an implicit function of M_3, which we then numerically solve and get M_3^*. Comparing the four components in the expression of V_f with Eqs. (7), (9), (11), (12) and (13) we can see that V_f is indeed the total energy, with M_3 replaced by M_3^* representing the higher torsion due to excess link added. In the smooth situation where there is no friction, any excess link results in the lengthening of the plectoneme so M_3 always remains at the plateau. But when there is a barrier, excess link accumulates, raises M_3 (which we distinguish by denoting as M_3^*) and finally raises the total free energy V_f. A plot of V_f as a function of $\triangle L_p$ for different $\triangle n$ is given in Fig. 3a. For each fixed $\triangle n$, V_f is convex and decreasing near $\triangle L_p = 0$, and we verify that $|\partial V_f/\partial\triangle L_p|$ increases as more turns are added. This causes a flattening of the local minima as shown in Fig. 3b.

View Article Online
DOI: 10.1039/C8SM00852C

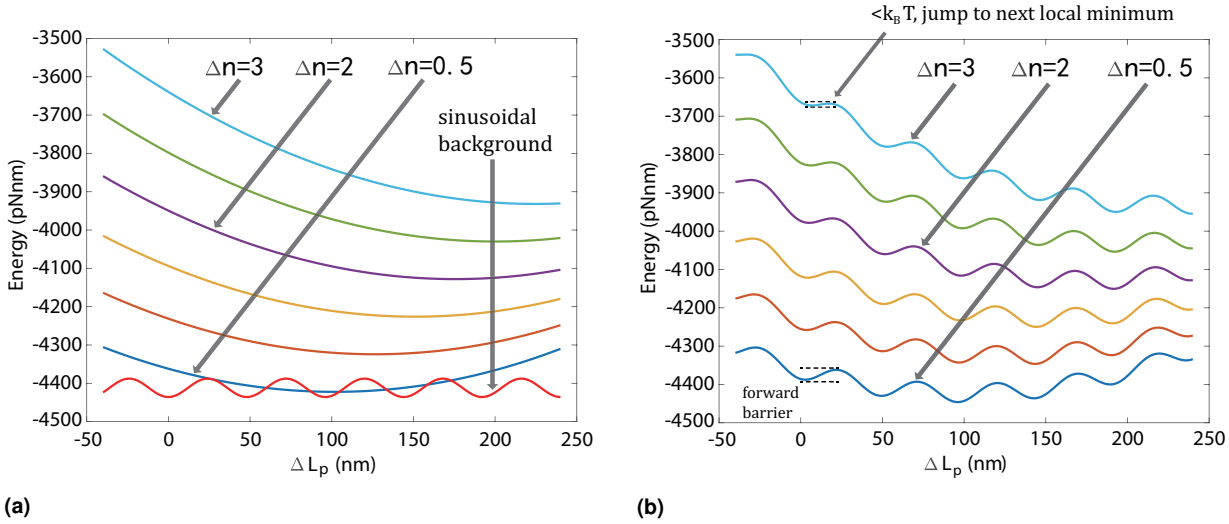

Fig. 3 (a) The sinusoidal curve represents the corrugated energy field (the first term in the RHS of Eq. 19). The convex curves represent a temporal sequence of V_f in Eq.19, where a higher curve corresponds to a larger value of $\triangle n$. We can see as $\triangle n$ increases, the slope $|\partial V_f/\partial \triangle L_p|$ around $\triangle L_p = 0$ increases rapidly. (b) Corresponding temporal sequence of V_{tot} for different values of $\triangle n$, which is produced by adding the sinusoidal function with each convex function V_f. The increase in the slope $|\partial V_f/\partial \triangle L_p|$ when $\triangle n$ increases results in the flattening of the local minimum which is initially located at $\triangle L_p = 0$.

To be specific, we call the energy barrier from the first local minimum to the second local minimum the *forward* barrier, and from the second to the first minimum a *backward* barrier. We see that eventually the height of the forward barrier approaches k_BT, and a jump (or slip) happens due to thermal effects. In stick-slip motion it is important that the reverse jump does not happen. This is also predicted by our model, since the height of the backward barrier is always several times larger than k_BT during the loading process (Fig. 3a), which suggests a negligible probability of a reverse jump compared with a forward jump[37,38].

Note that in the model with friction, $\triangle L_p$ can be viewed as a function of $\triangle n$. This is because $\triangle L_p$ always stays at a local minimum during the process when $\triangle n$ increases. Therefore, in the plectonemic regime, $\triangle L_p$ has a discontinuous response to increasing $\triangle n$. This is the reason behind the phenomenon that the end-to-end distance has stick-slip type of behavior as applied turns n increases[6] (Fig.4a). As a result, we can view M_3^* as a function solely of $\triangle n$. Unlike the model without friction in which M_3 remains constant as $\triangle n$ is increased, M_3^* is approximately a periodic function of $\triangle n$ when friction is present. In each period (or 'stick'), $\triangle L_p$ doesn't change as $\triangle n$ increases, thus the moment in the whole filament M_3^* increases as extra turns are stored as twist. Once M_3^* reaches some critical value at which the forward barrier described above approaches k_BT, $\triangle L_p$ jumps to the next local minimum. This results in a growth of the plectoneme, and the extra number of turns are stored as writhe in the plectoneme, which causes M_3^* to jump to the lower critical value, i.e., the plateau value predicted by the model without friction. The overall value of M_3^* thus always remains in a fixed range between these two critical values. A plot of M_3^* against applied turns is given in Fig.4b.

2.4 Sizes of the jumps

We have shown that there are two related periodic processes. First, the moment M_3^* looks like a periodic function of $\triangle n$ after the plectonemic transformation, and each period is characterized by a jump from a larger critical value to a lower critical value. Second, the corresponding rotation-extension curve has periodic jumps. Let n_{step} denote the number of turns in one period for both processes (since they are the same period). Then, n_{step} is the number of turns needed to induce a jump, and corresponds with the horizontal step size as in Fig 4a. Another step size in the same figure is the vertical step size (with units 'nm'), which we denote by l_{step}. This corresponds to the shortening of the tails, or equivalently the increased length of plectoneme in each period. From analysis of the P-T model we know that the increase in the length of the plectoneme is almost always equal to the period of the sinusoidal background. Therefore $l_{step} = \rho a$ where ρ is given by Eqn (18). n_{step} and l_{step} together determine the geometry of the stair-step curve in Fig 4a.

We now give quantitative detail about n_{step}. Let $\triangle B$ denote the forward energy barrier, which can be computed numerically from Eq.19. The estimation of n_{step} in our model is given by the solution of

$$\triangle B = k_BT, \tag{25}$$

which means a jump will happen due to thermal fluctuations once the forward barrier reaches k_BT[37,38]. From Eq.19 $\triangle B$ depends on $\triangle n$ and $\triangle L_p$. Therefore, the step size n_{step} varies slightly as total applied turns n increases.

In the model of Argudo and Purohit[6], the slope of the rotation-extension curve (in absolute value) is given by

$$\rho \frac{dL_p}{dn} = \rho \left(\frac{\sin 2\theta}{4\pi r} - \frac{M_3}{8\pi K_b K} \right)^{-1}. \tag{26}$$

View Article Online
DOI: 10.1039/C8SM00852C

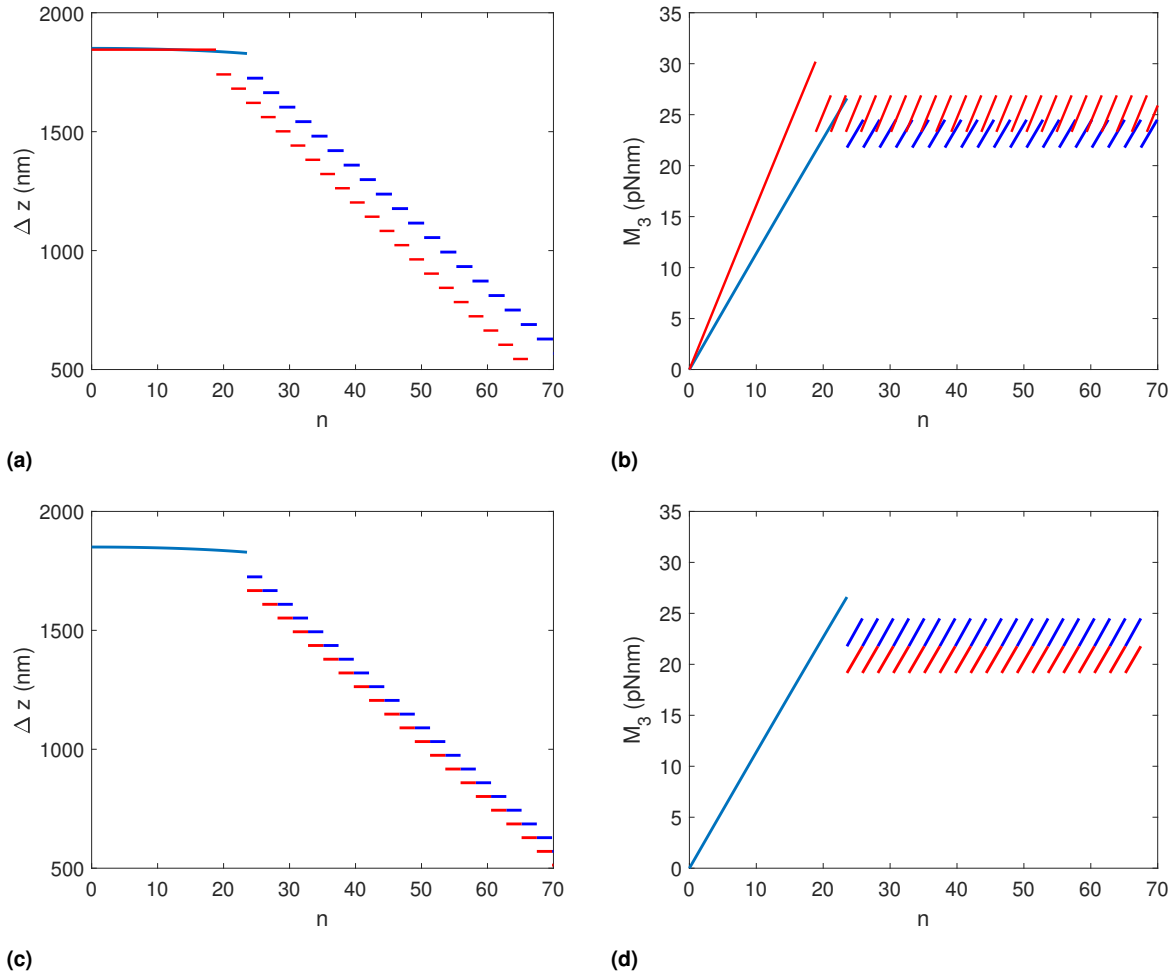

Fig. 4 (a) Theoretical plot of the rotation-extension curve under $F = 3.6$ pN and $c_0 = 0.5$ [M], as the applied turns n increases. After the plectoneme transition, the decrease in the end-to-end length is discontinuous. The red and blue curves stand for two different choices of stiffness K_b and K_t. Increasing K_b and K_t for the blue curve by a factor of 1.4 generates the red curve. (b) Theoretical plot of rotation-torque curve. After the transition, the torque looks like a periodic function of the applied turns n, and it varies within a fixed range. The lower bound is given by the plateau torque in the model without friction. The upper bound is calculated using n_{step}. The blue and red curves here have the same meaning as in Fig. 4a. (c) The blue curve is the same rotation-extension curve as in Fig. 4a and the red curve here corresponds to unloading, i.e., when applied turns n is decreased. The loading and unlodaing curves are different; thus, there is hysteresis. (d) Blue and red curves are the respective rotation-torque curves for the loading and unloading curves in Fig. 4c. Again, hysteresis is clear.

This indicates that the step size n_{step} must satisfy the following:

$$n_{step} = l_{step} \left(\rho \frac{dL_p}{dn} \right)^{-1}. \tag{27}$$

Hence, in the sinusoidal energy field, the period a and amplitude U_0 are related.

The analysis above assumes the existence of a single plectoneme in twisted DNA which is realistic for high ion concentrations ($\geq 0.3M$) as shown by Loenhout *et al.*[31], especially for tensions $F \geq 1$pN. Most experiments of Dittmore and Neuman in which discontinuous plectoneme growth is seen are in this high ion concentration high tension regime. However, Matek *et al*[39] and Medalion and Rabin[40] have shown that multiple plectonemes can be formed in supercoiled DNA if a few soft domains (such as, short AT rich domains) are introduced. Experimental evidence for the nucleation of plectonemes at a local 10-nt mismatched sequence (which is a soft domain) has been given in Ganji *et al.*[41] and experimental evidence for multiple plectonemes at ion concentrations larger than 0.15M is given in Loenhout *et al.*[31]. In the presence of multiple plectonemes the average slope of the rotation-extension curve after buckling given by ρ in eqn. (18) is not affected because it depends only on the applied tensile force F, the mechanical properties of the DNA (K_b, for example) and ion concentration which determines the interaction potential in the plectoneme. Thus, the ratio between the n_{step} and l_{step} (given by eqn. (27)) which characterizes the stair-step pattern remains independent of the number of coexisting plectonemes. Now, n_{step} is determined by the condition that the forward energy barrier ΔB becomes equal to k_BT (eqn. (25)). If there are p plectonemes then there are p such energy barriers because there are p contact points. Let us assume now that a plectoneme has just grown by l_{step} and the torque $M_3{}^* = M_3$ is at the lower value in the plateau.

View Article Online
DOI: 10.1039/C8SM00852C

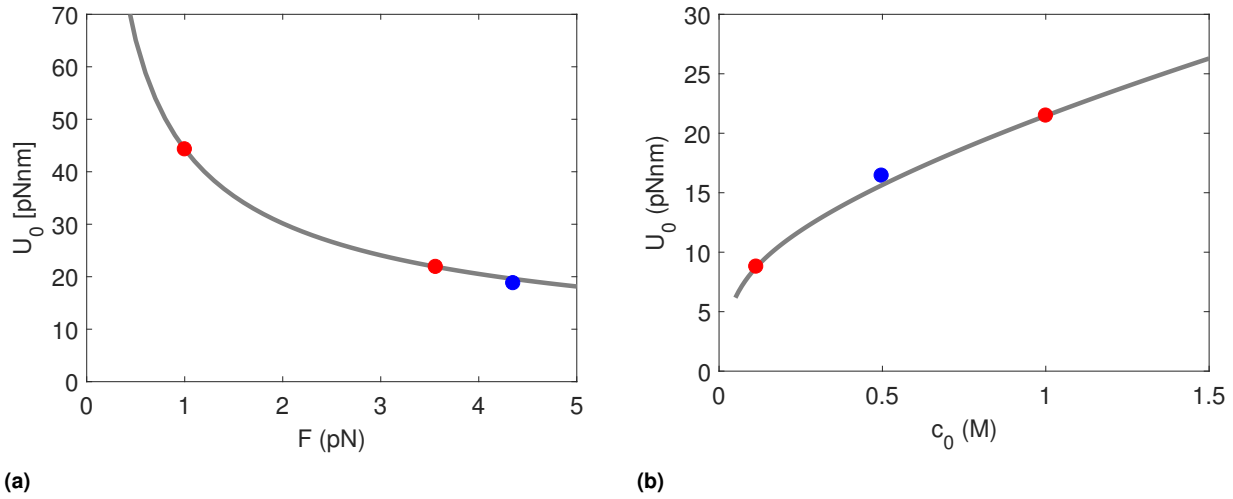

Fig. 5 (a) Models and comparison with experimental data for different tensile forces F. Three data points from Dittmore and Neuman[13] are marked by dots. The grey curve is fitted using two data points marked by red dots. The third data point marked by a blue dot is very close to the curve. A least squares fit of the three data points yields $\alpha = -0.5697$ and $m = 44.33$ for the amplitude of the corrugated potential $U_0 = mF^{\alpha}$ when c_0 is fixed at 1[M]. (b) Models and comparison with experimental data over different ionic concentration c_0. Three data points from Dittmore and Neuman[13] are marked by dots. The grey curve is fitted using two data points marked by red dots. The third data point marked by a blue dot is very close to the model-predicted curve. A least squares fit of the three data points yields $\beta = 1.933$ and $k = 35.81$ in $U_0 = \frac{k}{(r(c_0))^{\beta}}$ when F is fixed at 3.6 pN.

If the number of turns is held fixed then the forward and backward energy barriers for each plectoneme are similar (see figure 3b above) and they may grow/shrink in such a way as the total link is fixed as seen in the experiments of Loenhout *et al.*[31]. As more turns are added the torque $M_3{}^*$ increases because the twist in the DNA increases while the writhe in the plectonemes remains almost the same. Hence, the backward energy barrier increases and the forward energy barrier decreases (see figure 3b above). When $M_3{}^*$ reaches a high enough value that the forward barrier ΔB for each plectoneme is near k_BT then a random thermal fluctuation will cause *one* of the plectonemes to grow because its forward barrier is surmounted. The probability of multiple barriers being surmounted at the same time instant is small. As soon as one plectoneme grows, the torque $M_3{}^*$ again goes back to the lower plateau value M_3 to restart another cycle. In other words, the rotation-extension curve and rotation-torque curve for multiple coexisting plectonemes should look the same as if there was just one plectoneme.

Next, let us consider sequence dependent stiffness. Vlijm *et al.*[42] have suggested that the bending energy of plectonemes and the torsional modulus of DNA increase with increasing GC content. This will affect the mechanics through eqns. (19)-(24). We have tried to gain insight into this effect by incresing both K_b and K_t in our model by a factor of 1.4 (to model increased stiffness due to increased GC content) while keeping U_0 fixed (it depends on tension and ion concentration, see below). The results for the rotation-extension and rotation-torque curve are plotted as the red curves in figure 4a and figure 4b. Qualitatively, increasing the stiffness of the DNA moves the rotation-extension curve to the left, and the rotation-torque curve to higher torques.

Finally, let us consider what happens when we unload, (i.e.) when n is decreased. We assume again that the plectoneme has just grown and the torque M_3^* is at the lower plateau value corresponding to the bottom of an energy well. When n is decreased the energy landscape tilts the other way (opposite to that shown in figure 3b), so that the forward energy barrier grows and the backward energy barrier becomes smaller. The torque M_3^* now decreases below the lower plateau value because the twist in the tails decreases while the writhe in the plectonemes does not change much. Eventually, the backward energy barrier is flattened and the plectoneme shrinks to bring M_3^* to the lower plateau value. As n is decreased further the process repeats. The resulting rotation-extension and rotation-torque curves for unloading are plotted in red in figure 4c and figure 4d, respectively, along with the curves for loading in blue. Hysterisis is evident in figure 4d. This hysterisis arises due to the corrugated energy landscape whose amplitude is U_0 and is a prediction of our model.

From the above analysis we see that the parameter that affects the step size in the jump is the amplitude of the corrugated background potential U_0. This amplitude largely depends on the distance between the two interacting strands in the contact region, which in our case depends of the tensile force F and ionic concentration c_o[43]. An exact expression of U_0 as a function of F and c_o remains unknown, although a form in terms of F and the plectoneme radius r (which depends on F and c_0) has been suggested by Dittmore and Neuman[13]. We propose an expression with $U_0 \propto f(c_0) \times F^{\alpha}$, which is used to fit the experimental data from Dittmore and Neuman[13] and generates good results in section 3. This expression can be used for further predictions. Other functional forms of U_0 can also be plugged into our model and be tested against the experimental results of Dittmore and Neuman[13].

View Article Online
DOI: 10.1039/C8SM00852C

3 Comparison with experiments and prediction

We first focus on the relation between U_0 and F. In the experiment of Dittmore and Neuman[13], the data for various values of F are available at fixed ionic concentration $c_0 = 1[M]$. At fixed ionic concentration, the step sizes n_{step} and l_{step} are measured for three different values of F. Therefore, we need to numerically compute U_0 from the data of n_{step} by using Eqn.(25). In more detail, recall that for a given U_0, its corresponding n_{step} is the number of extra turns needed to induce a jump, which happens when Eqn.(21) is satisfied. This means if the value of n_{step} is given instead, the corresponding U_0 can be determined.

To find the value of the parameters m and α in $U_0 = mF^{\alpha}$ for a fixed ion concentration, we need two experimental data points which are available from Dittmore and Neuman[13]. Computation shows $U_0 \propto F^{-0.5548}$ when $c_0 = 1[M]$ (i.e. $\alpha = -0.5548$). The result of our model after fitting the parameters is shown in Fig.5a. We use two data points to fit the model and get the value of the parameters m and α and show in Fig.5a that our prediction for the third point matches the experiment quite well. A least squares fit of all three data points yields $\alpha = -0.5697$ when $c_0 = 1[M]$. With the quantitative relation between the amplitude U_0 in the P-T-like argument and the force F being clear, we are able to predict how step sizes (n_{step} and l_{step}) depend on F, since n_{step} is the critical extra link that satisfies Eqn.25. Once n_{step} is known, l_{step} is computed from the slope of the rotation-extension curve which is known from eqn. (26). The results are shown in Fig.6a for n_{step} vs. F and Fig.6b for l_{step} vs. F. Experimental data from the measurements of Dittmore and Neuman[13] are shown with error bars. The gray curves in both figures are model predictions which are in good agreement with experiment.

When F instead of c_0 is fixed, we have $U_0 \propto f(c_0)$. Our expression of $f(c_0)$ considers the interaction between the two strands at the contact region (i.e. the region between the tails and the plectoneme). We conjecture that the dependence of U_0 on ion concentration will be determined by electrostatics, so we propose a model with $U_0 \propto 1/z^{\beta}$, where z is the distance between the segments of strands in the contact region as we defined above. For example, $\beta = 1$ for two point charges with no mobile ions. We assume $f(c_0) = k/z^{\beta_1}$ for some constant k. Although we know qualitatively that z is a decreasing function of c_0, the quantitative dependence of z on c_0 is by far unknown to our knowledge. However, we do have the quantitative result of how the plectonemic radius r varies for different c_0 from numerical computation[6]. Therefore, we propose that $z \propto r^{\beta_2}$ for some constant β_2. Let $\beta = \beta_1\beta_2$. Then,

$$U_0 \propto \frac{1}{r^{\beta}} = \frac{k}{(r(c_0))^{\beta}}. \tag{28}$$

As with the force dependence of U_0, there are two parameters to be fitted. We use two data points to fit the parameter and use the third one to test our quantitative model. We get $U_0 \propto r^{-1.9826}$. The result is shown in Fig.5b. The two points with red color are used for fitting, and the third blue point falls nearly exactly on the curve. A least squares fit of all three data points yields $\beta = 1.933$ for $F = 3.6$pN. With the dependence of U_0 on c_0 known, our model can predict the quantitative relation between the step size and the ionic concentration. The result for n_{step} is shown in Fig.6c and the result for l_{step} is shown in Fig.6d. Experimental data with error bars are shown in the figure. The grey curve is the result of model prediction which is in good agreement with the experiment.

Combining the results for force dependence and ionic concentration dependence, we get the final expression

$$U_0 \propto (r(c_0))^{-1.9826}\, F^{-0.5548}. \tag{29}$$

In hindsight, the scaling $U_0 \sim F^{-0.5}$ suggests that the energy barrier is proportional to the size of the contact region which scales as $F^{-0.5}$ if we assume it to be similar in length to the loop formed just after the plectoneme transition[5,23].

4 Conclusion

We have explored the possibility of the existence of friction during the process of plectoneme formation in DNA. Specifically, we seek a model to explain the discontinuities (jumps) in the growth of a plectoneme in the experiments of Dittmore and Neuman[13]. We find that a Prandtl-Tomlinson model can explain the experimental data both qualitatively and quantitatively. The key in the P-T argument is to introduce a periodic corrugated energy potential, which causes an energy barrier that prevents the plectoneme from growing smoothly when extra turns are added. To explain the existence of this corrugated background potential, we qualitatively study the motion of the DNA filaments in the contact region. When the ionic concentration is high, the distance between the two strands becomes small and close to the DNA diameter. Qualitatively, this makes it possible for friction forces to come into play. Then, the periodicity of the background potential can be attributed to the periodic rotational motion of the two strands in the contact region[34,35] – as turns are added the angle between the strands changes in a periodic manner, and the periodicity is closely related with the step (n_{step}) needed to induce a jump. Due to the existence of peaks in the corrugated potential which act as energy barriers, the growth of the plectoneme is not a smooth process. A different qualitative explanation (with some similar features as our model) for the existence of these energy barriers has also been given by Dittmore and Neuman[13]. When enough free energy is accumulated in the DNA to flatten the barrier, a jump can happen due to thermal fluctuation. This idea is known as stick-slip motion in the classical P-T model[16,32,33]. The data of Dittmore and Neumann[13] seems to show similar stick-slip-type behavior. We show that an analysis based on the classical P-T model combined with the physics of DNA can fully explain the experimental observations of Dittmore and Neuman[13]. In fact, we have shown that the presence of a corrugated energy landscape can lead to different rotation-extension and rotation-torque curves for loading and unloading leading to hysterisis. This is a prediction from our model that can be tested in single molecule experiments.

Our analysis could be extended to other rod-like molecules. For example, plectonemes are formed in dsRNA[44] and actin filaments under the action of myosin X motors[45]. Since both dsRNA and

View Article Online
DOI: 10.1039/C8SM00852C

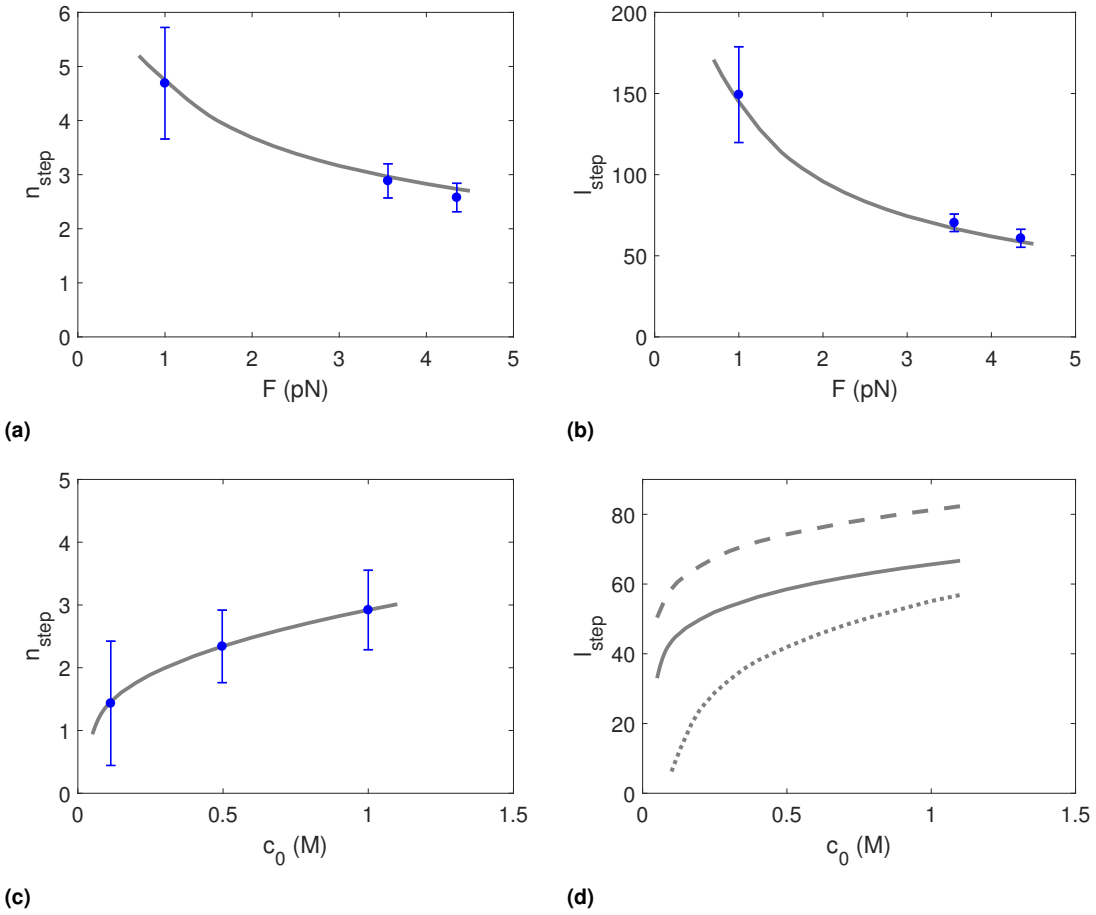

Fig. 6 (a) Our model and experimental data from Dittmore and Neuman[13] for different tensile forces F. Three data points of n_{step} with error bars under different tensile forces are marked. The grey curve is the prediction of our model, which is generated using the dependence of U_0 on F and c_0 (see Fig.5a). (b) Models and data for different tensile forces F. Three data points of l_{step} under different tensile forces with error bars from Dittmore and Neuman[13] are marked. The grey prediction curve is generated by using the dependence of n_{step} on F Fig.6a) and the slope of rotation-extension curve. (c) Models and data of n_{step} for different values of ionic concentration c_0 and F fixed at 3.6pN. (d) The solid curve is corresponding l_{step} computed from curve for n_{step} in Fig.6c. The other two curves are plotted by choosing values for α and β different from fitted value: the dashed curve at the top uses $\alpha = -0.3$ while keeping β the same as the fitted value; the dotted curve at the bottom uses $\beta = 3$ while keeping α as fitted.

actin are charged helical polymers plectonemes in them are likely to respond similarly (i.e. friction may be important) to those in dsDNA under high ion concentrations and high tensions. More generally, the Prandtl-Tomlinson model of solid-like friction has already been demonstrated to be important in the sliding of microtubules, bacterial flagella and actin filaments by Ward *et al*[43] who control the distance between neighboring filaments (and hence the frictional behavior) by changing depletant and ion concentrations. Ward *et al.* emphasize the importance of sliding friction described by the P-T model in the macroscopic deformations of biofilament bundles.

The next interesting question is the quantitative dependence of the step size on tensile force F and ionic concentration c_0, which has been studied experimentally in the experiment of Dittmore and Neuman[13]. Within the classical P-T model the step size is controlled by the amplitude U_0 and period a in the corrugated potential. Hence, we must determine how U_0 changes as F and c_0 change. In the experiment of Dittmore and Neuman[13], data for step size variation with varying force F (ionic concentration c_0) is collected at fixed c_0 (F). While Dittmore and Neuman[13] suggest a dependence of U_0 on F, we use the step size to compute the corresponding U_0. We propose a model in which the energy barrier U_0 is proportional to a certain power of F, where the power is determined through fitting data. Such a power law dependence of energy on force has been used in Loenhout *et al.*[31] to study the diffusion (which is related to friction) of plectonemes along DNA. In particular, the diffusion of plectonemes along DNA involves slithering motion between the two strands of the plectoneme and fluid drag on the plectoneme as a whole. The diffusion coefficient in[31] is not explained by the drag on the plectoneme; rather it is assumed in[31] that diffusion is retarded by a factor $g(\varepsilon) = \exp(-(\frac{\varepsilon}{k_B T})^2)$ where $\varepsilon \propto \sqrt{F}$ is the fluctuating part of the energy landscape and F is the tension. In Loenhout *et al.*[31] the fluctuating part of the energy landscape is assumed to be random and could arise from microscopic causes including sequence dependence. In contrast, in our model we find after fitting experimental data that the amplitude U_0 of a corrugated energy landscape varies as $U_0 \propto F^{-0.5548}$ which is close to $F^{-1/2}$. Since

View Article Online
DOI: 10.1039/C8SM00852C

it is known[5] that the length of the contact region scales as $F^{-1/2}$ we surmise in hindsight that the size of the energy barrier might depend linearly on the length of the contact region. Note that in contrast to Loenhout *et al.*[31] (a) our energy landscape is not random, it is periodic, and (b) its amplitude may be only wealkly dependent on sequence because the energy landscape has to do with the relative rotational motion of two pieces of DNA that come into contact at a point. The dependence of U_0 on c_0 is more complicated. Since U_0 is likely to be dominated by electrostatic interactions between the two strands in the contact region, we propose a model in which U_0 is proportional to a certain power of the reciprocal of the distance between two strands. With these ingredients our model accurately predicts the experimental data. However, a more rigorous analysis (experiment, computations and theory) is required to determine the nature of U_0.

Conflicts of interest

There are no conflicts to declare.

Acknowledgements

We thank Andrew Dittmore and Keir Neuman for providing us their experimental data and for discussions regarding the physics of plectoneme formation. Our thanks are also due to Jonathon Silver, who participated in these discussions, and to Paul Wiggins, who brought this problem to our attention. We acknowledge partial support for this work from a United States National Science Foundation grant NSF CMMI 1662101 and from the National Institutes of Health via grant NIH R01-HL 135254.

Notes and references

1 P. Nelson, *Biological physics*, WH Freeman New York, 2004.
2 W. Fraser and D. Stump, *International journal of solids and structures*, 1998, **35**, 285–298.
3 B. D. Coleman and D. Swigon, *Journal of elasticity and the physical science of solids*, 2000, **60**, 173.
4 S. Goyal, N. C. Perkins and C. L. Lee, *Journal of Computational Physics*, 2005, **209**, 371–389.
5 P. K. Purohit, *Journal of the Mechanics and Physics of Solids*, 2008, **56**, 1715 – 1729.
6 D. Argudo and P. K. Purohit, *Acta Biomaterialia*, 2012, **8**, 2133 – 2143.
7 S. Goyal, T. Lillian, N. C. Perkins and E. Meyhofer, *arXiv:physics/0702197*, 2007.
8 J. Lipfert, J. W. Kerssemakers, T. Jager and N. H. Dekker, *Nature methods*, 2010, **7**, 977–980.
9 F. Mosconi, J. F. Allemand, D. Bensimon and V. Croquette, *Physical review letters*, 2009, **102**, 078301.
10 C. Maffeo, R. Schöpflin, H. Brutzer, R. Stehr, A. Aksimentiev, G. Wedemann and R. Seidel, *Physical review letters*, 2010, **105**, 158101.
11 H. Brutzer, N. Luzzietti, D. Klaue and R. Seidel, *Biophysical Journal*, 2010, **98**, 1267–1276.
12 S. Goyal, N. C. Perkins and J.-C. Meiners, *Journal of Computational and Nonlinear Dynamics*, 2008, **3**, 011003.
13 A. Dittmore and K. C. Neuman, *arXiv:physics/1804.06442*, 2018.
14 N. Clauvelin, B. Audoly and S. Neukirch, *Biophysical journal*, 2009, **96**, 3716–3723.
15 S. Neukirch and J. F. Marko, *Physical review letters*, 2011, **106**, 138104.
16 E. Gnecco and E. Meyer, *Fundamentals of Friction and Wear on the Nanoscale*, Springer, 2015.
17 M. G. Poirier, A. Nemani, P. Gupta, S. Eroglu and J. F. Marko, *Physical review letters*, 2001, **86**, 360.
18 M. G. Poirier and J. F. Marko, *Physical review letters*, 2002, **88**, 228103.
19 R. Arun and S. Ghosal, *Physics Letters A*, 2017, **381**, 2386–2390.
20 S. Ghosal, *Physical review letters*, 2012, **109**, 248105.
21 M. Nizette and A. Goriely, *Journal of mathematical physics*, 1999, **40**, 2830–2866.
22 J. D. Moroz and P. Nelson, *Macromolecules*, 1998, **31**, 6333–6347.
23 I. M. Kulić, H. Mohrbach, R. Thaokar and H. Schiessel, *Physical Review E*, 2007, **75**, 011913.
24 J. Ubbink and T. Odijk, *Biophysical journal*, 1999, **76**, 2502–2519.
25 J. Marko and E. Siggia, *Physical Review E*, 1995, **52**, 2912.
26 J. R. Van der Maarel, *Introduction to biopolymer physics*, World Scientific, 2008.
27 D. Andelman, *Soft condensed matter physics in molecular and cell biology*, 2006, **6**, year.
28 P. K. Purohit, IUTAM Symposium on Cellular, Molecular and Tissue Mechanics, 2010, pp. 123–138.
29 J. D. Moroz and P. Nelson, *Proceedings of the National Academy of Sciences*, 1997, **94**, 14418–14422.
30 R. R. Sinden, C. E. Pearson, V. N. Potaman and D. W. Ussery, *Advances in genome biology*, 1998, **5**, 1–141.
31 M. T. van Loenhout, M. de Grunt and C. Dekker, *Science*, 2012, **338**, 94–97.
32 L. Prandtl, *Z. Angew. Math. Mech*, 1928, **8**, 85–106.
33 G. Tomlinson, *The London, Edinburgh, and Dublin philosophical magazine and journal of science*, 1929, **7**, 905–939.
34 D. Stump, W. Fraser and K. Gates, 1998, **454**, 2123–2156.
35 D. Stump and W. Fraser, 2000, **456**, 455–467.
36 J. M. T. Thompson and A. Champneys, *Proc. R. Soc. Lond. A*, 1996, **452**, 117–138.
37 E. Riedo, E. Gnecco, R. Bennewitz, E. Meyer and H. Brune, *Physical review letters*, 2003, **91**, 084502.
38 K. Jinesh, S. Y. Krylov, H. Valk, M. Dienwiebel and J. Frenken, *Physical Review B*, 2008, **78**, 155440.
39 C. Matek, T. E. Ouldridge, J. P. Doye and A. A. Louis, *Scientific reports*, 2015, **5**, 7655.
40 S. Medalion and Y. Rabin, *The Journal of Chemical Physics*, 2016, **144**, 135101.
41 M. Ganji, S. H. Kim, J. van der Torre, E. Abbondanzieri and C. Dekker, *Nano letters*, 2016, **16**, 4699–4707.
42 R. Vlijm, J. vd Torre and C. Dekker, *PloS one*, 2015, **10**,

View Article Online
DOI: 10.1039/C8SM00852C

e0141576.

43 A. Ward, F. Hilitski, W. Schwenger, D. Welch, A. Lau, V. Vitelli, L. Mahadevan and Z. Dogic, *Nature materials*, 2015, **14**, 583–588.

44 J. Lipfert, G. M. Skinner, J. M. Keegstra, T. Hensgens, T. Jager, D. Dulin, M. Köber, Z. Yu, S. P. Donkers, F.-C. Chou *et al.*, *Proceedings of the National Academy of Sciences*, 2014, **111**, 15408–15413.

45 S. Nagy, B. L. Ricca, M. F. Norstrom, D. S. Courson, C. M. Brawley, P. A. Smithback and R. S. Rock, *Proceedings of the National Academy of Sciences*, 2008, **105**, 9616–9620.